Mechanized silica nanoparticles based on reversible bistable [2]pseudorotaxanes as supramolecular nanovalves for multistage pH-controlled release

ARTICLE *in* CHEMICAL COMMUNICATIONS · APRIL 2014

Impact Factor: 6.83 · DOI: 10.1039/c4cc01442a · Source: PubMed

4 AUTHORS:

Mingdong Wang
Nanjing University of Science and Technology
6 PUBLICATIONS **76** CITATIONS
SEE PROFILE

Tao Chen
Nanjing University
9 PUBLICATIONS **193** CITATIONS
SEE PROFILE

Chendi Ding
Nanjing University of Science and Technology
3 PUBLICATIONS **32** CITATIONS
SEE PROFILE

Jiajun Fu
Nanjing University of Science and Technology
26 PUBLICATIONS **386** CITATIONS
SEE PROFILE

ChemComm

COMMUNICATION

View Article Online
View Journal

Mechanized silica nanoparticles based on reversible bistable [2]pseudorotaxanes as supramolecular nanovalves for multistage pH-controlled release†

Cite this: DOI: 10.1039/c4cc01442a

Received 25th February 2014,
Accepted 25th March 2014

DOI: 10.1039/c4cc01442a

www.rsc.org/chemcomm

MingDong Wang,‡ Tao Chen,‡ ChenDi Ding and JiaJun Fu*

Cucurbit[6]uril-based reversible bistable [2]pseudorotaxanes were designed, synthesized and installed on the surface of mesoporous silica nanoparticles as supramolecular nanovalves. The assembled mechanized silica nanoparticles realize the multistage pH-controlled release of benzotriazole and the potential for reutilization.

Mechanized silica nanoparticles (MSNPs), which are composed of mesoporous silica nanoparticles as scaffolds and mechanically interlocked molecules as supramolecular nanovalves, are capable of accommodating and releasing cargo molecules on demand and have received great attention due to their potential applications in the field of stimuli-responsive controlled drug delivery systems and intelligent anticorrosion coatings.[1,2] As the key part of MSNPs, supramolecular nanovalves, usually in the form of [2]pseudorotaxanes and bistable [2]rotaxanes, undergo the relative mechanical movement between their ring components and threads on the nanoscale, by which MSNPs can encapsulate the cargo molecules within the mesopores under normal conditions and release them in response to environmental changes, such as pH, redox potential, light, biomolecules, *etc.*[3–6]

In the past decade, a multitude of supramolecular nanovalves based on [2]pseudorotaxanes have been designed and fabricated. The transition states of nanovalves from "closed" to "open" are mainly caused by the gradually weak supramolecular interactions between the macrocycles and the linear stalks anchored on the surface of mesoporous silica nanoparticles upon external stimuli. However, after accomplishing release missions, the complete structures of MSNPs are broken owing to the dethreading of macrocyclic gatekeepers from the linear stalks.[7] As comparison, making use of bistable [2]rotaxanes as nanovalves not only actualizes multistage controlled release in a "release–halt–release" way, but also achieves another important objective for reloading and reusing of MSNPs by the reciprocating motion of macrocycles on the linear stalks. To our knowledge, investigations of bistable [2]rotaxanes to realize reversible switching function are still rare. Stoddart and Zink *et al.* attached the bistable [2]rotaxanes covalently to the surface of MCM-41 and finish a cycle for loading and releasing of guest molecules, in which cyclobis(paraquat-*p*-phenylene) ($CBPQT^{4+}$) macrocycles shuttled between the tetrathiafulvalene (TTF) stations and the dioxynaphthalene (DNP) stations under redox control.[8] Lately, they have designed light-triggered reversible nanovalves based on the azobenzene α-cyclodextrin system.[9]

Herein, we introduce a novel design for MSNPs based on mesoporous silica nanoparticles equipped with the reversible bistable [2]pseudorotaxanes to control pore access. The molecular structure of the bistable [2]pseudorotaxane, which contains 1,6-hexanediammonium (HDA) and 1,6-bis(pyridinium)hexane (BPH) as two recognition sites, as well as cucurbit[6]uril (CB[6]) as macrocycles are shown in Scheme 1. In this interlocked molecule, CB[6] macrocycles can be switched between two distinct recognition sites according to pH changes. Under neutral or acidic solution, the CB[6]

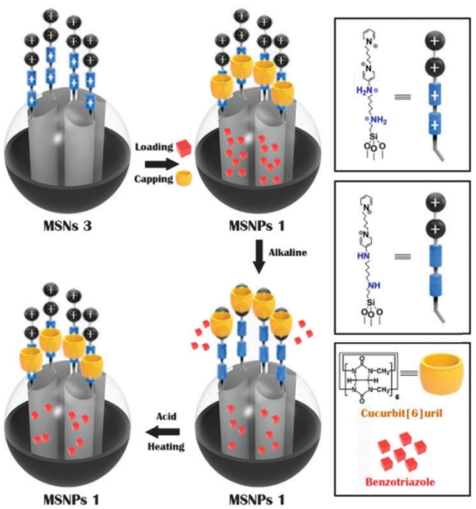

Scheme 1 Schematic representation of operation of the MSNPs **1**.

School of Chemical Engineering, Nanjing University of Science and Technology, Nanjing, China. E-mail: fujiajun668@gmail.com; Fax: +86 025 84315609; Tel: +86 025 84315609

† Electronic supplementary information (ESI) available: Experimetal details and analytical data. See DOI: 10.1039/c4cc01442a

‡ These authors contributed equally to this article.

macrocycles choose to stay on the HDA stations rather than the BPH stations, preventing cargo molecules escape. When the pH value turns to alkaline, the ammonium moieties of HDA are deprotonated and the binding affinity between CB[6] macrocycles and HDA stations is weakened, which leads to the migration of CB[6] macrocycles from the HDA recognition stations to the BPH stations far away from the entrance of the pores. At this moment, the nanovalves are opened and the cargo molecules are free to diffuse out. If the pH of solution is adjusted from alkaline to weak acidic conditions once more, the CB[6] macrocycles originally recognized on the BPH stations will shuttle back to the HDA stations, which facilitates the well-designed MSNPs fulfil the multistage pH-controlled release and therefore, can be recycled and reused.

MCM-41-type mesoporous silica nanoparticles (MSNs) were synthesized according to the previous literature and used as starting nanocarriers.[10] Transmission electron microscopy, small-angle X-ray powder diffraction, and N_2 adsorption–desorption isotherms demonstrate that the monodispersed, diameter of about 150 nm nanospheres have hexagonal channels with an average pore diameter of 2.65 nm and a surface area of 1118 $m^2\ g^{-1}$ (Fig. S2, ESI†). The assembly process of MSNP **1** is depicted in Fig. S1 (ESI†). The as-prepared MSNs were first functionalized with (3-aminopropyl) trimethoxysilane to obtain MSNs **1**, which were then treated with 1,6-dibromohexane to give MSNs **2**. After that, the MSNs **2** were reacted with compound **1** (the detailed synthesis process is provided in the ESI†) to yield MSNs **3**. To obtain MSNPs **1**, the MSNs **3** were loaded with 1*H*-benzotriazole (BTA), which is chosen as the probe molecule and capped with CB[6] macrocycles.

Three-step functionalization processes are confirmed through Fourier transform infrared (FTIR) spectroscopy. As shown in Fig. 1, MSNs only show the various Si–OH and Si–O–Si vibrations, while MSNs **1** exhibit an absorption band at 2930 cm^{-1}, which corresponds to the C–H stretching vibration. Compared with MSNs **1**, a new absorption band at 580 cm^{-1}, a characteristic stretching band of the C–Br bond is shown in the FTIR spectrum of MSNs **2**. After coupled with compound **1**, the intensity band of C–Br bond is considerably reduced, and the absorption peaks at 1500–1400 cm^{-1} appear due to the pyridine skeleton vibration, indicating the successful attachment of organic stalks on the exterior surfaces of

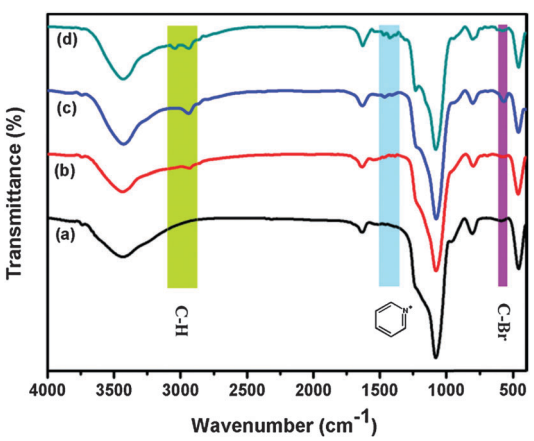

Fig. 1 FTIR spectra of pure MSNs (a), MSNs **1** (b), MSNs **2** (c), and MSNs **3** (d).

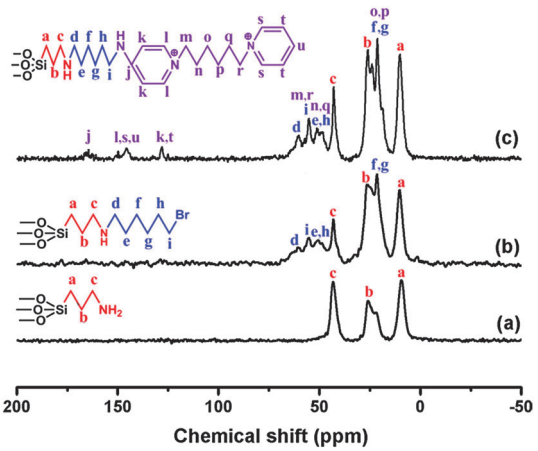

Fig. 2 ^{13}C CP-MAS solid-state NMR spectra of MSNs **1** (a), MSNs **2** (b), and MSNs **3** (c).

MSNs. The ^{13}C CP-MAS solid-state NMR spectra of MSNs **1**, MSNs **2** and MSNs **3** are illustrated in Fig. 2 and provide further evidence of functionalization. The NMR spectrum of MSNs **1** shows three resonance signals at 10, 26 and 43 ppm that can be attributed to the peaks of carbon a, b, and c of 3-aminopropyl group. In the NMR spectrum of MSNs **2**, apart from the peaks of carbons a, b and c, some new intense signals were observed at 22, 51, 55, 60 ppm, corresponding to the carbons f–g, e–h, i and d on the hexyl chain. As for MSNs **3**, the additional three resonance signals appearing around 128, 146 and 160 ppm can be assigned to the characteristic aromatic carbons (k–t, l–s–u and j) of the pyridine groups, indicating the formation of the second recognition sites, BPH stations, which is also proved by the ^{29}Si CP-MAS solid-state NMR spectra (Fig. S3, ESI†).

X-ray photoelectron spectroscopy (XPS) is also used to verify the introduction of the intact stalks inside the framework of MSNs. The apparent differences between MSNs **3** and MSNs (Fig. S4, ESI†) are in the presence of N 1s and C 1s signals in the XPS spectrum of MSNs **3**, but not detected in the MSNs. From thermogravimetric analysis data as shown in Fig. S5 (ESI†), when MSNs are successively functionalized with (3-aminopropyl) trimethoxysilane, 1,6-dibromohexane and compound **1**, the approximate total weight loss is 11.5 wt% (about 0.86 mmol g^{-1} MSNs), 8.5 wt% (about 0.5 mmol g^{-1} MSNs), and 7.4 wt% (about 0.42 mmol g^{-1} MSNs), respectively. Although the intensity of the diffraction peak, the specific surface area and the pore volume are inevitably decreased after each step of functionalization, this does not greatly influence the adsorption capacity of mesoporous materials (Fig. S6 and S7, ESI†).

After installation of the planned stalks, the MSNPs **1** were assembled. Three different measurement methods were adopted to investigate the operation modes of MSNP **1** in detail. First of all, Fig. 3 shows release profiles by plotting the absorbance intensity of BTA at 265 nm from the MSNPs **1** in response to different pH as a function of time. The leakage of BTA at pH 7.0 was negligible (less than 1.2% total amount of the adsorbed BTA), revealing that the entrance of pores were blocked by CB[6] macrocycles. But in the alkaline solution, the UV/Vis absorbance

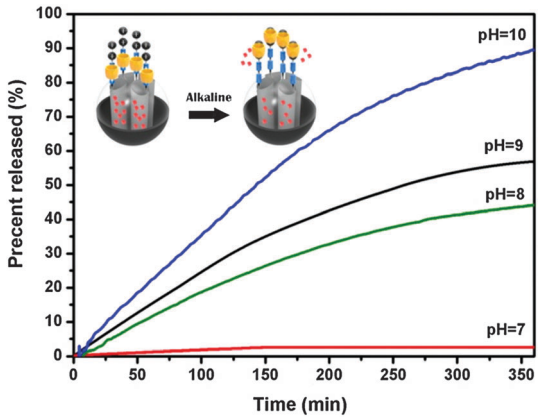

Fig. 3 Release profiles of BTA from MSNPs **1** at different pH values.

of BTA increased immediately, manifesting the rapid escape of BTA from MSNPs **1**. Furthermore, the release rate is obviously dependent on the alkalinity of solution. The stronger the alkalinity is, the higher deprotonation degree of HDA units is, the more numbers of CB[6] macrocycles detached from the HDA stations there are, and the more rapid the release rate we observe.

In the condition of near neutral or acidic solution, CB[6] macrocycles are threaded onto the HDA stations due to that the stability constant for the host–guest complex between CB[6] and HDA units is more than that between CB[6] and BPH units.[11] As solution alkalinity is increased, 1,6-hexanediammonium are gradually in the deprotonated form.[12] The high binding affinity of complex HDA⊂CB[6] dramatically declines, the CB[6] macrocycles cannot reside on the HDA stations and transfer to the BPH stations where the complex formation of BPH⊂CB[6] is little affected by pH values. In order to validate the reversibility of the moving process of CB[6] macrocycles, the second step, the multistage pH-controlled release experiment was conducted. As depicted in Fig. 4a, there was almost

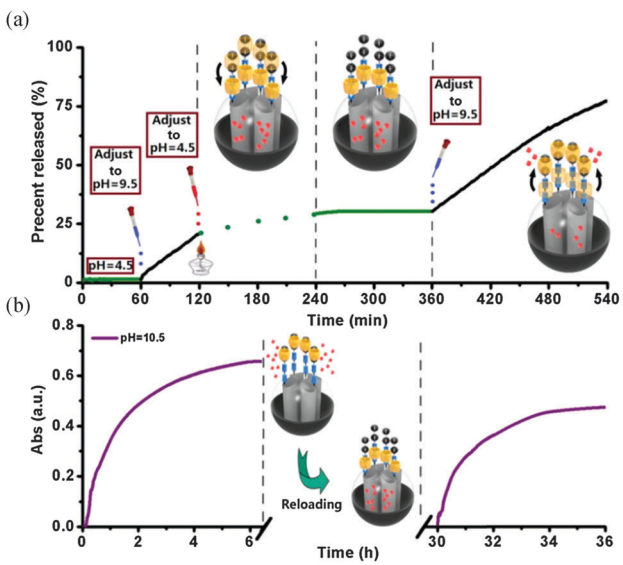

Fig. 4 Multistage pH-controlled release of BTA from MSNPs **1** (a) and reloading experiment of MSNPs **1** (b).

no leakage of BTA under pH 4.5. When the releasing process lasted for 60 min under pH 9.5, the pH of solution was readjusted to 4.5, simultaneously supplemented by heating solution to 45 °C for 2 h. After that, the release process was found to be shut off and the concentration of benzotriazole in solution was very stable through continuous monitoring, demonstrating that CB[6] macrocycles shuttled back to the HDA stations and restarted to regulate the guest molecules diffusing in or out of the MSNPs **1**.

Based on the anticipative results of the multistage pH-controlled experiment, the reloading ability of MSNPs **1** was finally investigated. The approximately complete release of BTA was performed at pH 10.5 for 12 h. The reloading procedure is similar to the initial adsorption experiment. The re-collected MSNPs **1** were suspended in 15 mg mL^{-1} aqueous BTA solution at pH 10.5 for 12 h, which ensures the encirclement of CB[6] macrocycles on the BPH stations during the reloading process, and then closed the nanovalves, washed for the second release measurement. As shown in Fig. 4b, the pH-controlled release profile for the second cycle exhibits the similar features as that from the first cycle. However, the reloading capacity is less than 20% for the first cycle, which may be attributed to the space steric effect of CB[6] macrocycles.

In summary, a new type of MSNPs with the reversible bistable [2]pseudorotaxanes as supramolecular nanovalves has been developed. The one-dimensional piston movement of CB[6] macrocycles between the HDA and the BPH stations guarantee the reversible switching activity of nanovalves. The operational mechanisms make MSNPs **1** open or close repeatedly at the molecular lever in response to the pH stimulus, which will expand their application area.

This research was financially supported by the National Natural Science Foundation of China (No. 51102135), the Natural Science Foundation of Jiangsu Province (No. BK2011711), the 2013-ZiJin-0102 Talent Program, NUST, and Jiangsu Graduate Innovation Project (No. CKLX13_196).

Notes and references

1 (*a*) K. K. Coti, M. E. Belowich, M. Liong, M. W. Ambrogio, Y. A. Lau, H. A. Khatib, J. I. Zink, N. M. Khashab and J. F. Stoddart, *Nanoscale*, 2009, **1**, 16; (*b*) M. W. Ambrogio, C. R. Thomas, Y. L. Zhao, J. I. Zink and J. F. Stoddart, *Acc. Chem. Res.*, 2011, **44**, 903; (*c*) P. P. Yang, S. L. Gai and J. Lin, *Chem. Soc. Rev.*, 2012, **41**, 3679.

2 (*a*) T. Chen and J. J. Fu, *Nanotechnology*, 2012, **23**, 235605; (*b*) T. Chen and J. J. Fu, *Nanotechnology*, 2012, **23**, 505705; (*c*) J. J. Fu, T. Chen, M. D. Wang, N. W. Yang, S. N. Li, Y. Wang and X. D. Liu, *ACS Nano*, 2013, **7**, 11397.

3 (*a*) M. Xue, X. Zhong, Z. Shaposhnik, Y. Q. Qu, F. Tamanoi, X. F. Duan and J. I. Zink, *J. Am. Chem. Soc.*, 2011, **133**, 8798; (*b*) Y. L. Zhao, Z. X. Li, S. Kabehie, Y. Y. Botros, J. F. Stoddart and J. I. Zink, *J. Am. Chem. Soc.*, 2010, **132**, 13016; (*c*) S. Angelos, N. M. Khashab, Y. W. Yang, A. Trabolsi, H. A. Khatib, J. F. Stoddart and J. I. Zink, *J. Am. Chem. Soc.*, 2009, **131**, 12912; (*d*) T. Chen, N. W. Yang and J. J. Fu, *Chem. Commun.*, 2013, **49**, 6555.

4 (*a*) R. Liu, X. Zhao, T. Wu and P. Y. Feng, *J. Am. Chem. Soc.*, 2008, **130**, 14418; (*b*) G. Q. Silveira, M. D. Vargas and C. M. Ronconi, *J. Mater. Chem.*, 2011, **11**, 6034.

5 (*a*) Y. L. Sun, B. J. Yang, S. X. A. Zhang and Y. W. Yang, *Chem. – Eur. J.*, 2012, **18**, 9212; (*b*) H. Yan, C. Teh, S. Sreejith, L. L. Zhu, A. Kwok, W. Q. Fang, X. Ma, K. T. Nguyen, V. Korzh and Y. L. Zhao, *Angew. Chem., Int. Ed.*, 2012, **51**, 8373; (*c*) S. Angelos, Y. W. Yang, N. M. Khashab, J. F. Stoddart and J. I. Zink, *J. Am. Chem. Soc.*, 2009, **131**, 11344.

6 (*a*) Y. L. Sun, Y. Zhou, Q. L. Li and Y. W. Yang, *Chem. Commun.*, 2013, **49**, 9033; (*b*) S. S. Wu, X. Huang and X. Z. Du, *Angew. Chem., Int. Ed.*, 2013, **52**, 5580.

7 (*a*) D. P. Ferris, Y. L. Zhao, N. M. Khashab, H. A. Khatib, J. F. Stoddart and J. I. Zink, *J. Am. Chem. Soc.*, 2009, **131**, 1686; (*b*) C. Wang, Z. X. Li, D. Cao, Y. L. Zhao, J. W. Gaines, O. A. Bozdemir, M. W. Ambrogio, M. Frasconi, Y. Y. Botros and J. I. Zink, *Angew. Chem., Int. Ed.*, 2012, **51**, 5460.
8 (*a*) T. D. Nguyen, H. R. Tseng, P. C. Celestre, A. H. Flood, Y. Liu, J. F. Stoddart and J. I. Zink, *Proc. Natl. Acad. Sci. U. S. A.*, 2005, **19**, 10029; (*b*) S. Saha, K. C. F. Leung, T. D. Nguyen, J. F. Stoddart and J. I. Zink, *Adv. Funct. Mater.*, 2007, **17**, 685.
9 D. Tarn, D. P. Ferris, J. C. Barnes, M. W. Ambroqio, J. F. Stoddart and J. I. Zink, *Nanoscale*, 2014, **6**, 3335.
10 C. Y. Hong, X. Li and C. Y. Pan, *J. Mater. Chem.*, 2009, **19**, 5155.
11 (*a*) J. W. Lee, K. P. Kim and K. Kim, *Chem. Commun.*, 2001, 1042; (*b*) L. Yuan, R. B. Wang and D. H. Macartney, *J. Org. Chem.*, 2007, **72**, 4539.
12 (*a*) J. S. Liu and X. Z. Du, *J. Mater. Chem.*, 2010, **20**, 3642; (*b*) S. Angelos, Y. W. Yang, K. Patel, J. F. Stoddart and J. I. Zink, *Angew. Chem., Int. Ed.*, 2008, **47**, 2222.

